Geofísica Internacional (2017) 56-2: 173-186

Original paper

Guadalajara, Mexico, Earthquake Sequence of December 2015 and May 2016: Source, *Q*, and Ground Motions

Shri Krishna Singh*, Danny Arroyo, Xyoli Pérez-Campos, Arturo Iglesias, Víctor Hugo Espíndola and Leonardo Ramírez with contributions by Citlalli Pérez and Héctor Sandoval

Received: August 12, 2016; accepted: February 28, 2017; published on line: April 01, 2017

Resumen

Se analizó una secuencia de sismos que se produjo a 24 km NNW de la catedral de Guadalajara. La actividad inició el 15 de diciembre de 2015, con un sismo de M_w4.1 y se reanudó el 11 de mayo de 2016, cuando ocurrió el sismo más grande de la secuencia, M_w4.8. Los sismos fueron registrados por dos acelerógrafos en la ciudad y por estaciones de banda ancha a distancias mayores. La región de la fuente de la secuencia se encuentra en el norte de la amplia unión formada por los *rifts* Tepic-Zacoalco, con una orientación NW-SE, el de Colima, con una tendencia N-S, y el de Chapala, con tendencia E-W. El mecanismo focal del evento más grande se caracteriza por: rumbo φ = 21º, echado δ = 49º, y deslizamiento λ = -86º, con el eje de tensión horizontal en una dirección 110º. Este mecanismo no es consistente con la dirección NE-SW de movimiento medido en un echado de falla por Barrier *et al*. (1990) ~ 35 km al WNW de Guadalajara. También se diferencia del mecanismo reportado en un estudio previo para una secuencia sísmica en el *rift* de Zacoalco unos 60 km al sur de Guadalajara. La similitud de las formas de onda en las estaciones acelerográficas sugiere que el mecanismo de otros eventos en la secuencia fueron similares y los eventos se localizan en un volumen pequeño, probablemente en un radio de 1 a 2 km. A partir del análisis de registros del sismo del 11 de mayo a lo largo de la Faja Volcánica Trans Mexicana, desde el volcán Ceboruco, hacia el oeste, y hasta el volcán Popocatépetl, al este, se estimó el parámetro de atenuación Q como $141f^{0.63}$. El sismo del 11 de mayo se sintió fuertemente en la ciudad y produjo una aceleración máxima del terreno (*PGA*) que alcanzó 80 cm/s^2. En la región se han reportado sismos relativamente grandes; e.g., 11 de febrero de 1875 en San Cristóbal de la Barranca, por lo cual resulta de interés emplear los registros de las estaciones acelerográficas para estimar los parámetros pico del movimiento del terreno debidos a escenarios sísmicos con $M_w \leq 6.0$ utilizando la teoría de vibraciones aleatorias (RVT) y las técnicas de la función de Green empírica (EGF). A partir de simulaciones empleando RVT, los valores de *PGA* esperada, velocidad pico (*PGV*) y desplazamiento pico (*PGD*) del movimiento del terreno en las estaciones acelerográficas para un sismo M_w6.0 en la región de la fuente de la secuencia son 195 cm/s^2, 10 cm/s y 3 cm, respectivamente. Las estimaciones obtenidas a partir de la técnica de EGF son más altas que las calculadas con RVT en un factor de no mayor de dos.

Palabras clave: secuencia de sismos de Guadalajara, valores pico de movimiento del terreno, peligro sísmico en Guadalajara.

S.K. Singh*
X. Pérez-Campos
A. Iglesias
V. H. Espíndola
Instituto de Geofísica
Universidad Nacional Autónoma de México
Ciudad Universitaria
Delegación Coyoacán, 04510
Mexico CDMX, México
*Corresponding author: krishna@geofisica.unam.mx

D. Arroyo
Departamento de Materiales
Universidad Autónoma Metropolitana
Mexico CDMX, México

L. Ramírez
C. Pérez
H. Sandoval
Instituto de Ingeniería
Universidad Nacional Autónoma de México
Ciudad Universitaria
Delegación Coyoacán, 04510
Mexico CDMX, México

Abstract

We analyze an earthquake sequence which occurred 24 km NNW from Guadalajara Cathedral. The activity began on 15 December, 2015 with an M_w4.1 earthquake and resumed, again, on 11 May, 2016 when the largest earthquake of the sequence, M_w4.8, occurred. The earthquakes were recorded in the city by two accelerographs and at larger distances by broadband seismographs. The source region of the sequence is located in the north of the broad junction formed by NW-SE trending Tepic-Zacoalco rift, N-S trending Colima rift, and E-W trending Chapala rift. The focal mechanism of the largest event is characterized by: strike φ = 21º, dip δ= 49º, and rake λ= -86º, with horizontal tensional axis trending 110º. This mechanism is not consistent with NE-SW direction of motion measured on fault strike by Barrier *et al*. (1990) ~ 35 km WNW of Guadalajara. It also differs from the mechanism reported in a previous study for a seismic sequence in the Zacoalco rift about 60 km south of Guadalajara. Similarities among recorded waveforms at the accelerographic stations suggest that the mechanism of other events in the sequence were similar and the events were located in a small volume, probably 1 to 2 km in radius. From the analysis of the recordings of the 11 May shock along the Trans-Mexican Volcanic Belt, from Ceboruco volcano to the west and Popocatepetl volcano to the east, the attenuation parameter Q as $141f^{0.63}$ was estimated. The earthquake on 11 May was felt very strongly in the city and produced peak ground acceleration (*PGA*) reaching 80 cm/s^2. Relatively large earthquakes have been reported in the region; e.g., on 11 February, 1875 near the town of San Cristobal de la Barranca, about 40 km NNW of Guadalajara, therefore, the interest on using recordings from accelerographic stations to estimate peak ground motion parameters for scenario earthquakes of $M_w \leq 6.0$ using random vibration theory (RVT) and empirical Green's function (EGF) techniques. From RVT simulations, the expected *PGA*, peak ground velocity (*PGV*), and peak ground displacement (*PGD*) at the accelerographic stations from an M_w6.0 earthquake in the source region of the sequence are 195 cm/s^2, 10 cm/s, and 3 cm, respectively. The predictions from the EGF technique are somewhat higher but still within a factor of two of the RVT predictions..

Key words: Guadalajara earthquake sequence, peak ground motion, Seismic hazard in Guadalajara.

Introduction

The Trans-Mexican Volcanic Belt (TMVB) is an east-west trending calc-alkaline volcanic arc related to the subduction of oceanic Rivera and Cocos plates below Mexico along the Middle America trench. The belt is traversed by networks of faults that are nearly parallel and orthogonal to its axis (e.g., Pasquaré *et al*., 1987; Johnson and Harrison, 1990; Suter *et al*., 2001). Seismicity in the TMVB is relatively low, and the seismic networks in the region are sparse. As a consequence, source parameters of earthquakes that occur in the TMVB, including their depths and focal mechanisms, are known for only a handful of earthquakes. The occurrence of large earthquakes in the TMVB is well documented. Acambay earthquake of 1912 (M_S7.0), which occurred in the central part of TMVB (Urbina and Camacho, 1913), about 100 km WNW of Mexico City, is one example. Jalapa earthquake of 1920 (M_w6.4), near the eastern end of the TMVB, caused many deaths related to a triggered landslide and was damaging to the city (Camacho and Flores, 1922). Suárez *et al*. (1994) report a large earthquake in 1568 (M~7) in/near Guadalajara in the western part of the TMVB which caused severe damage to the city. A relatively large earthquake occurred on 11 February, 1875 destroying the town of San Cristóbal de la Barranca located about 40 km NNW of Guadalajara (García Acosta and Suárez Reynoso, 1996). Clearly, cities and towns in the Mexican Altiplano are exposed to seismic hazard from earthquakes in the TMVB. A reliable estimation of this hazard, however, will only be possible by performing detailed studies of all well-recorded TMVB earthquakes; fortunately, the reported number of such events is increasing due to improvement in the seismic instrumentation of the region and quick deployment of digital portable seismographs in the field. As examples, recent well-studied earthquake sequences in the TMVB are cited, which occurred in Zacoalco, Jalisco (Pacheco *et al*., 1999), Sanfandila, Querétaro (Zúñiga *et al*., 2003), and Morelia, Michoacán (Singh *et al*., 2012).

In December 2015 and May 2016 an earthquake sequence occurred NNW of Guadalajara. The source region of the sequence is located to the north of the broad triple rift junction formed by NW-SE trending Tepic-Zacoalco, N-S trending Colima, and E-W trending Chapala rifts (Figure 1). The rifts of Tepic-Zacoalco and Colima are forming the northern and eastern boundaries of the Jalisco block which is separating from the North America plate. Active rifting is occurring

along these boundaries (e.g., Barrier *et al*., 1990; Allan *et al*., 1991; Michaud *et al*.,1994; Moore *et al*., 1994). The seismic sequence was recorded in the city by two accelerographs at an epicentral distance of about 20 km. The largest earthquake in the sequence (M_w4.8) occurred on 11 May, 2016, and was strongly felt in the city but caused no damage (R. Meli, personal communication, 2016). This event was also extensively recorded by the broadband seismographic network of the National Seismological Service (SSN). In this paper the source characteristics of some of the larger events of the sequence are studied and the attenuation parameter, Q, along central-west TMVB is estimated. Taking advantage of the recordings at the two accelerographic stations, an estimation of ground motions from scenario earthquakes of M_w5.5 and 6.0 in the source region of the sequence are performed. The results should be useful in seismic hazard estimation of Guadalajara from normal-faulting crustal earthquakes in the region.

Location, focal mechanism, and magnitude

As mentioned before, the sequence began on 15 December, 2015 with an earthquake of magnitude M_w4.1 located ~ 20 km NW of Guadalajara. SSN reported three more events in the next 40 hours. The activity resumed on 11 May, 2016 with a M_w4.8 earthquake, the largest event of the sequence. SSN reported 29 other events in the next 18 days. The closest SSN station which recorded these events was more than 100 km away and the *P* waves at the SSN stations were highly emergent. The sequence was also recorded by two accelerographs located on the campus of Universidad Panamericana (station GDLP) and Colegio Cervantes (station GDLC) (Figures 1 and 2). These stations are operated by Instituto de Ingeniería, UNAM. Recordings at these stations are made in continuous mode at 100 samples/s. Due to the noise level at these stations (especially at GDLC), very high during traffic hours at frequencies above about 8 Hz,

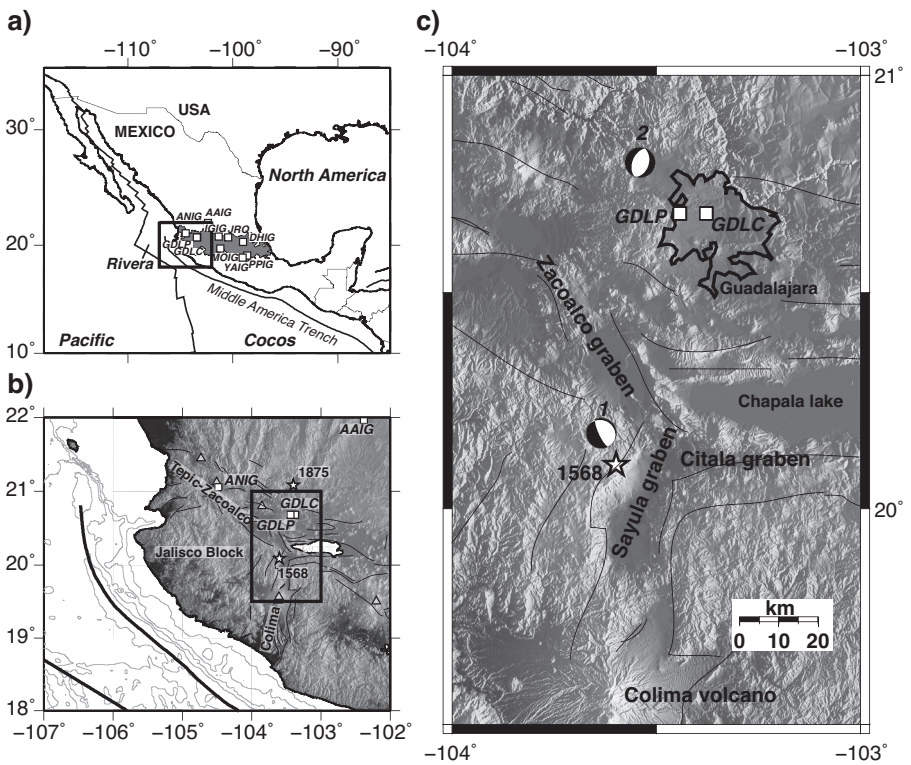

Figure1. a) Tectonic setting of the region. Gray area: Trans-Mexican Volcanic Belt. Rectangles: broadband stations in the belt which recorded 11 May, 2016 (M_w4.8) earthquake. Enlarged map of the area in the black rectangle is shown in b). b) Tectonic setting of west-central Mexico showing the Jalisco block and the rift-rift-rift triple point junction. Triangles: active volcanoes. Squares: accelerographic (GDLC and GDLP) and broadband (AAIG and ANIG) stations in the region. Stars correspond with the approximate epicenters for large historical earthquakes reported in the region. An enlarged view of the rectangular area, the region of interest, is shown on the right. c) Shaded relief map of the area around Guadalajara; its metropolitan area is enclosed within the black contour. Locations of seismic sequences of Zacoalco (1) and Guadalajara (2) are shown by their common focal mechanisms. Modified from Pacheco *et al*. (1999). Star corresponds with the approximate epicenter for the 1568 earthquake.

data are useful for $M \geq 3.0$ events only. However, a few earthquakes of smaller magnitudes also produced useful recordings when they occurred late at night or early in the morning. In total there were eight well-recorded events at these stations. These events, along with *PGA*, *PGV*, and *PGD* values, are listed in Table 1. We note that many historical monuments of the city, including the cathedral, are located only ~ 2 km eastward of the station GDLC (Figure 2). Hence, it is likely that the ground motions near these monuments were similar to those recorded at the station GDLC.

Figure 3 shows displacement seismograms at the station GDLP of six of the eight earthquakes listed in Table 1. The traces begin 0.5 s before the *P*-wave arrival. The vertical dotted lines in the top three frames indicate arrival of *P* and *S* waves. (*S*-*P*) time of the events which occurred during December 2015 is 2.5 s. The remarkable similarity of the waveforms and nearly the same (*S*-*P*) times of these events suggest nearly the same location and focal mechanism of these events. The bottom three frames correspond to the activity in May 2016. The largest shock of the sequence (11 May, 2016, M_w4.8) appears somewhat complex but still with (*S*-*P*) time of 2.5 s. Although the waveform of 15 May, 2016 event (bottom, second frame) differs somewhat from the others (probably reflecting its greater depth as reflected in the impulsive *P* wave), its (*S*-*P*) time is still about 2.5 s. The (*S*-*P*) time of the smallest event shown in the figure (bottom, third frame) is 0.1 s less than the others, suggesting its location ~1 km closer to the station than others.

The largest event of the sequence (11 May, 2016; 22:35) was located using *P* and *S* phases at the two local accelerographic stations and many broadband stations of SSN (distance > 100 km). Because of its size, this was the best-recorded event. Even so, the first motions could be read only at a handful of stations. The seismograms were converted to Seisan format (Havskov and Ottemöller, 1999) and the earthquake was located using the algorithm of Lienart and Havskov (1995) yielding the epicenter at 20.798 ºN, 103.539 ºW, with a poorly constrained depth of 8 km. Given the similarity of (*S*-*P*) times and the waveforms (Figure 3), we conclude that the earthquakes in Table 1 (and most of the events during the entire sequence) were tightly clustered, probably within a volume of 1 to 2 km radius.

The fault parameters of the 11 May, earthquake were determined by performing regional moment tensor (RMT) inversion using an algorithm implemented by A. Iglesias at the Servicio Sismológico Nacional (SSN, Mexican National Seismogical Service). The

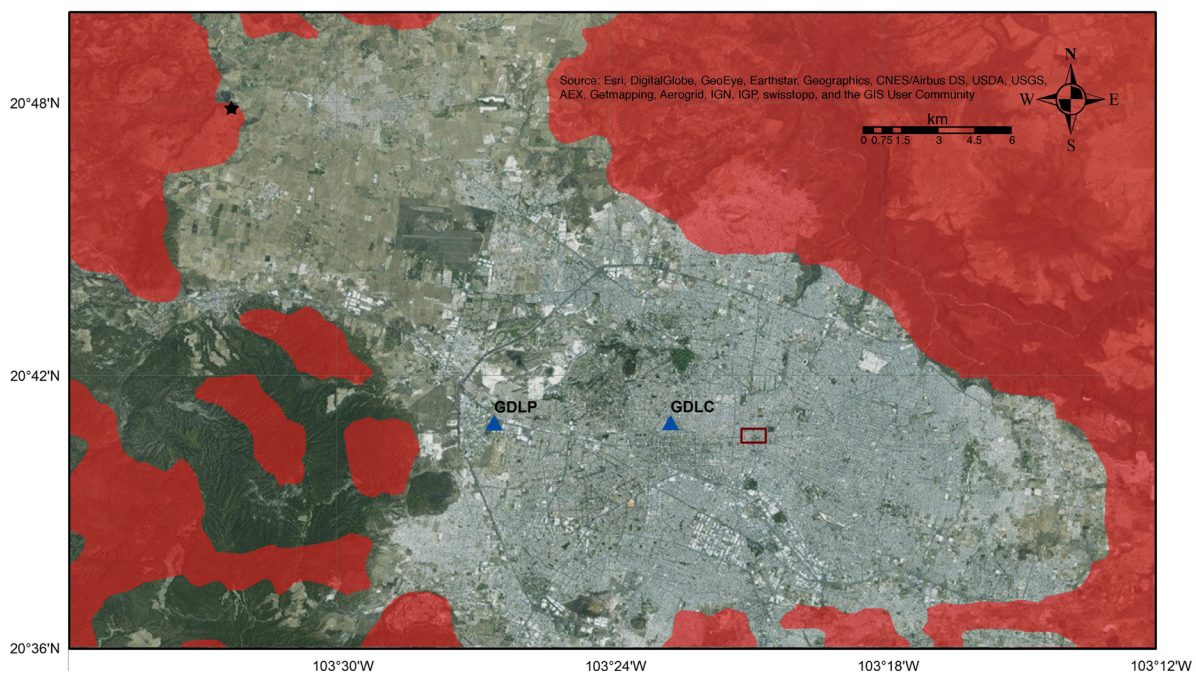

Figure 2. Map of Guadalajara and vicinity. Star: the epicenter of 11 May, 2016 (M_w4.8) earthquake. Triangles: accelerographic stations (GDLP and GDLC). Rectangle: area of famous monuments of the city. The red shaded area corresponds with presence of igneous intrusive rocks.

Table 1. *PGA*, *PGV*, and *PGD* of well-recorded events at two near-source stations ($R \sim 20$ km) during the December 2015 and May 2016 Guadalajara earthquake sequence.

			Station GDLP[1]			Station GDLC[2]		
			PGA cm/s^2 PGV cm/s PGD cm			PGA cm/s^2 PGV cm/s PGD cm		
Event number	Date Time	*M*w	NS	EW	Z	NS	EW	Z
1	2015-12-15 16:09	4.06	20.2 4.40E-01 2.70E-02	31.6 5.90E-01 4.50E-02	15.2 3.10E-01 1.60E-02	14.3 4.30E-01 4.20E-02	15.6 4.60E-01 3.70E-02	9.1 2.00E-01 1.00E-02
2	2015-12-15 16.32	2.88	3.7 6.30E-02 2.10E-03	4.1 6.70E-02 2.80E-03	2.5 4.70E-02 1.00E-03	- - -	- - -	- - -
3	2015-12-15 17:49	3.50	7.1 2.30E-01 1.30E-02	14.8 2.60E-01 1.90E-02	6.6 1.40E-01 9.10E-03	6.7 1.80E-01 1.30E-02	6.6 2.10E-01 1.60E-02	5.8 1.10E-01 4.20E-03
4	2015-12-17 7:59	3.50	15.3 3.60E-01 1.40E-02	17.3 5.30E-01 2.20E-02	12 2.30E-01 1.00E-02	6.7 1.70E-01 1.30E-02	7.3 2.20E-01 1.70E-02	6.6 1.70E-01 4.30E-03
5	2016-05-11 22:35	4.77	59.4 1.40E+00 7.70E-02	79.3 2.10E+00 2.10E-01	47.9 9.40E-01 3.50E-02	54.6 2.40E+00 1.40E-01	59 1.80E+00 1.90E-01	51.5 9.40E-01 6.70E-02
6	2016-05-15 1:43	3.15	1.9 5.50E-02 2.60E-03	1.56 5.10E-02 3.70E-03	1.95 4.50E-02 1.50E-03	1.57 4.90E-02 3.10E-03	1.58 4.10E-02 2.80E-03	1.56 3.80E-02 1.00E-03
7	2016-05-16 8:14	2.77	1.08 2.30E-02 8.30E-04	1.89 3.50E-02 1.80E-03	1.08 2.10E-02 4.90E-04	8.00E-01 1.40E-02 7.50E-04	1.12 2.10E-02 1.10E-03	6.80E-01 1.40E-02 4.00E-04
8	2016.05-29 6:40	2.88	7.70E-01 1.90E-02 7.90E-04	4.80E-01 1.30E-02 4.10E-04	7.30E-01 1.70E-02 4.10E-04	7.00E-01 1.90E-02 9.10E-04	3.50E-01 1.20E-02 6.00E-04	5.60E-01 1.20E-02 3.00E+04

[1]GDLP: Guadalajara, Universidad Panamericana.
[2]GDLC: Guadalajara, Colegio Cervantes.

method is described in some detail in UNAM Seismology Group (2010). System chooses appropriate broadband stations according to reported magnitude. Records from stations relatively close to the epicenter are discarded to avoid finite fault effects, and stations far from the epicenter are discarded to ensure good signal to noise ratio. Records of selected stations are integrated to obtain displacements and are band-pass filtered using frequencies that depend on magnitude criteria. This procedure tries to use low frequencies (where displacement spectrum is flat), avoiding high frequencies at which the structure is poorly known. Selected seismograms are inverted using a time domain scheme implemented by Dreger (2003). Computation time is dramatically reduced using a set of stored Green functions, which are computed at nodes of a grid of distances *vs*. depths and using an average *S*-wave velocity model. For Mexico, the SSN uses a model reported by Campillo *et al*. (1996).

The regional centroid moment tensor solution of the 11 May, earthquake reported by the SSN yields the following fault parameters: strike $\varphi = 21^{\circ}$, dip $\delta = 49^{\circ}$, strike $\lambda = -86^{\circ}$, and $M_0 = 1.8 \times 10^{16}$ Nm (M_w4.77). An inversion using a different combination of broadband stations $\varphi = 2^{\circ}$, $\delta = 49^{\circ}$, $\lambda = -123^{\circ}$, with $M_0 = 9.9 \times 10^{15}$ Nm (M_w4.60). As illustrated in Figure 4, both of these mechanisms are consistent with the first motion data; both show a nearly horizontal

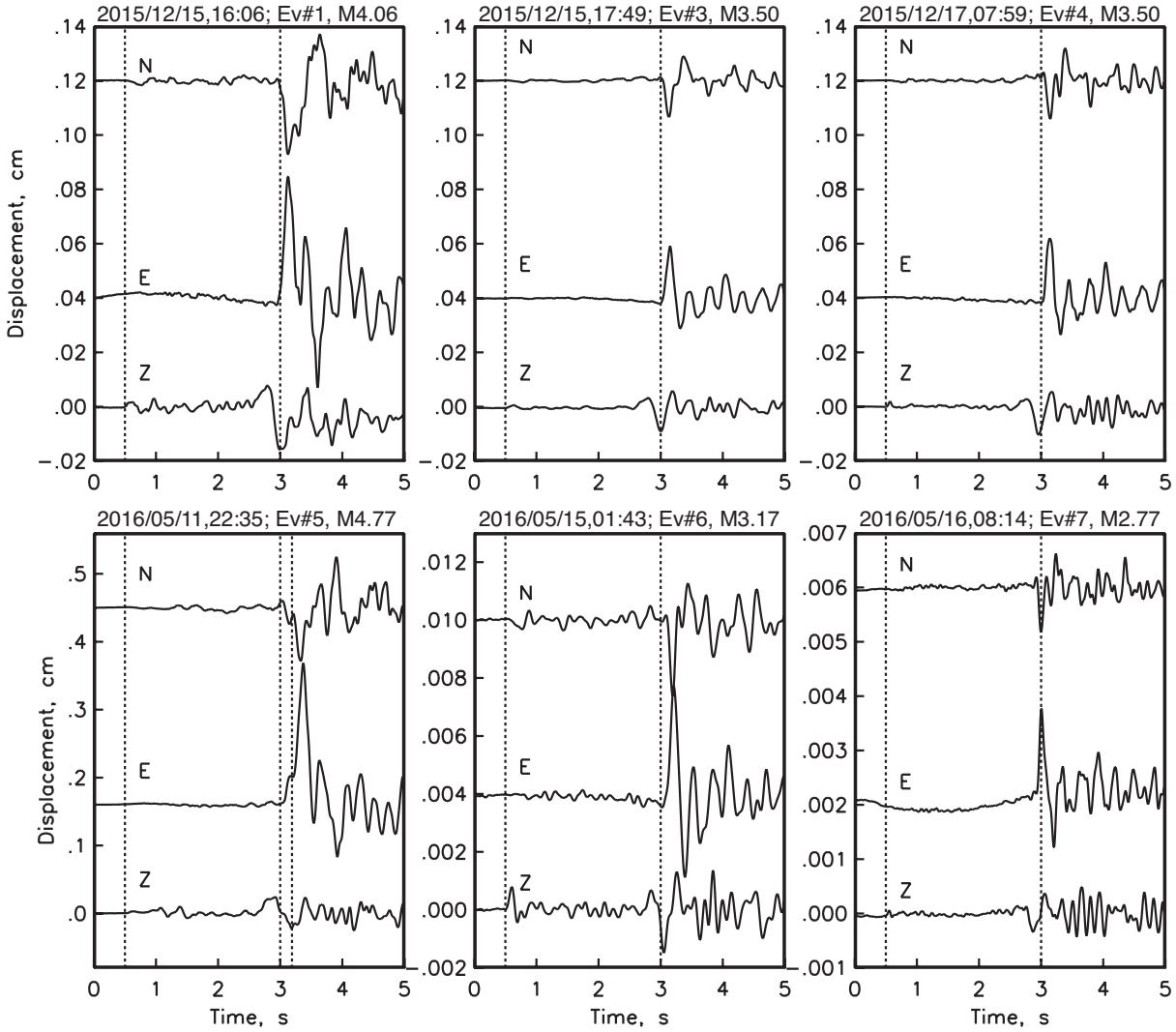

Figure 3. Displacement seismograms at the station GDLP of six of the larger earthquakes of the sequence which had clear signal at the station. Traces begin 0.5 s before *P*-wave arrival. Vertical dotted lines in the top three frames indicate the arrival of *P* and *S* waves, respectively. (*S*-*P*) time for these events, which occurred in December 2015, is 2.5 s. The remarkable similarity of the waveforms and nearly the same (*S*-*P*) times of these events suggest nearly the same location and focal mechanism of these events. The bottom three frames correspond to the activity in May 2016. The largest shock of this sequence appears complex but still with (*S*-*P*) of 2.5 s. Although the waveform of 15 May, 2016 event (second bottom frame) differs from others (probably reflecting its larger depth; note the impulsive *P* waves), its (*S*-*P*) time is still about 2.5 s. (*S*-*P*) time of the smallest event shown in the figure (bottom third frame) is 0.1 s less than the others, suggesting that it was located about 1 km closer to the station than others.

tensional axis trending ~ 110º. The figure also shows displacement traces of the earthquake at the station GDLP along with infinite space synthetics (Singh *et al*., 2000) corresponding to the two mechanisms. In these synthetics the effect of the free surface is approximately taken into account by multiplying infinite-space synthetics by two. The first solution above (φ = 21º, δ = 49º, λ = -86º) provides a better fit to the observed *S* pulse and is our preferred focal mechanism. We note that the mechanisms in Figure 4 differ from those reported 60 km to the south in the Zacoalco graben during the seismic sequence of 1997, which involved a NE-SW extension, consistent with the orientation of the rift (Pacheco *et al*., 1999).

To estimate the magnitudes of smaller events of the sequence listed in Table 1, Fourier acceleration spectra of the *Z*-component at the broadband station AAIG in Aguascalientes (Figure 1) was computed. All events listed in Table 1 were well recorded at this station. The spectra and the spectral ratios of 11

May, 20016 earthquake with respect to each of the other seven events are illustrated in Figures 5a and 5b, respectively. Taking the seismic moment of the 11 May earthquake as 1.8×10^{16} Nm, we estimated moments (hence M_w) of other events from the level of spectral ratios at low frequencies. Table 1 lists M_w of all events. If we take $M_0 = 9.9 \times 10^{15}$ Nm for the 11 May earthquake, as obtained from the second regional CMT solution, then M_w of all events will be 0.18 unit less.

Q along the Central-West TMVB

Attenuation parameter, Q, in the central and eastern TMVB has been studied by several authors. As discussed by Singh *et al*. (2007), the reported estimates of Q are inconsistent among the studies (see Figure 6). To our knowledge, no estimation of Q is available for the central-west segment of the TMVB.

The earthquake of 11 May, 2016 was recorded by eight broadband seismographs in the TMVB, extending from Ahuacatlán, near Ceboruco volcano (station ANIG) in the west and to Popocatepetl volcano (station PPIG) in the east, covering a distance range of about 650 km (Figure 1a). We use this dataset, along with the accelerograms in Guadalajara, to obtain a preliminary estimate of an average Q for the central-west TMVB. Note that we have included data from station AAIG in the analysis even though the wave path is not entirely through the TMVB. A procedure which has been used before in similar studies was used (e.g., Singh *et al*., 1982; Ordaz and Singh, 1992; García *et al*., 2004). Here the method is briefly described.

The Fourier acceleration spectral amplitude, $A(f, R)$, of the intense part of the ground motion of an event at distance R, considering the far-field point-source approximation, can be written as

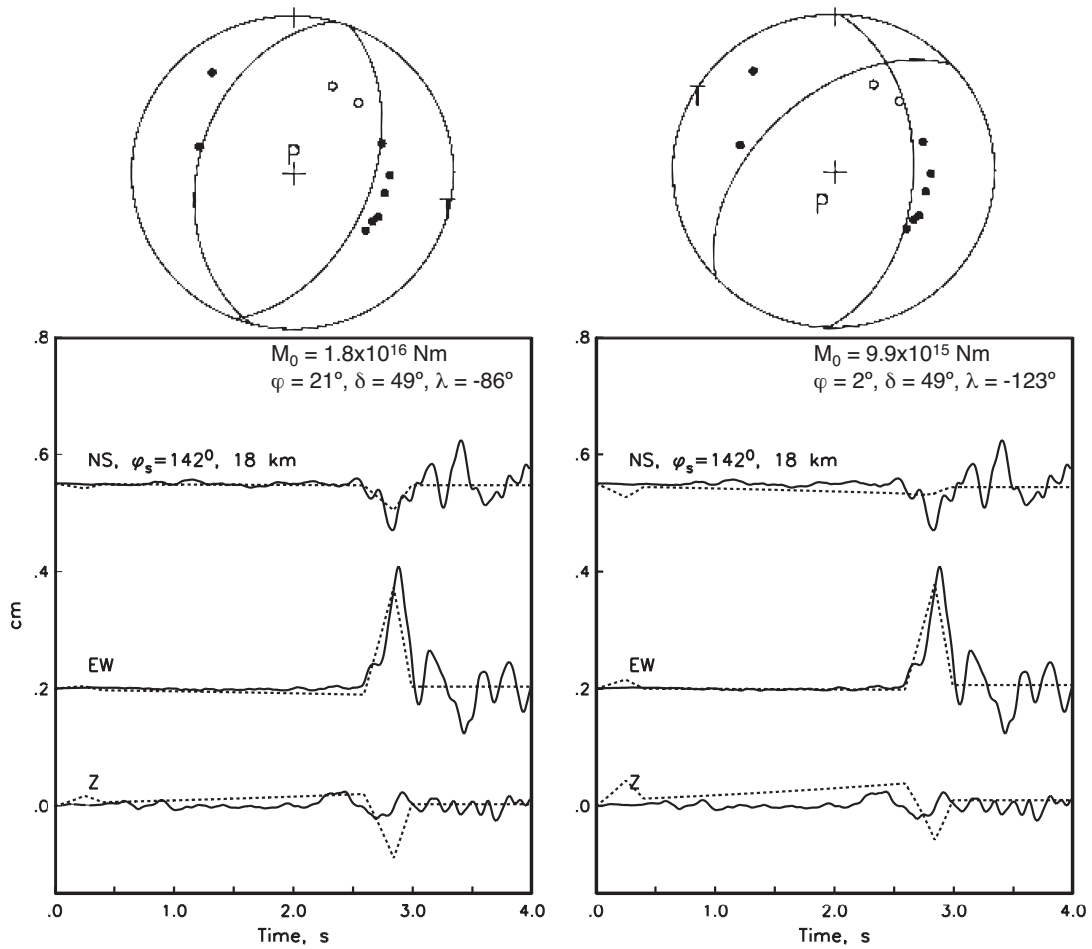

Figure 4. (Top) Focal mechanism of 11 May, 2016 earthquake. Two regional CMT solutions, using a different combination of broadband stations, are shown. First motions agree with both solutions. (Bottom) Displacement traces at station GDLP and infinite space synthetics corresponding to the two regional CMT solutions.

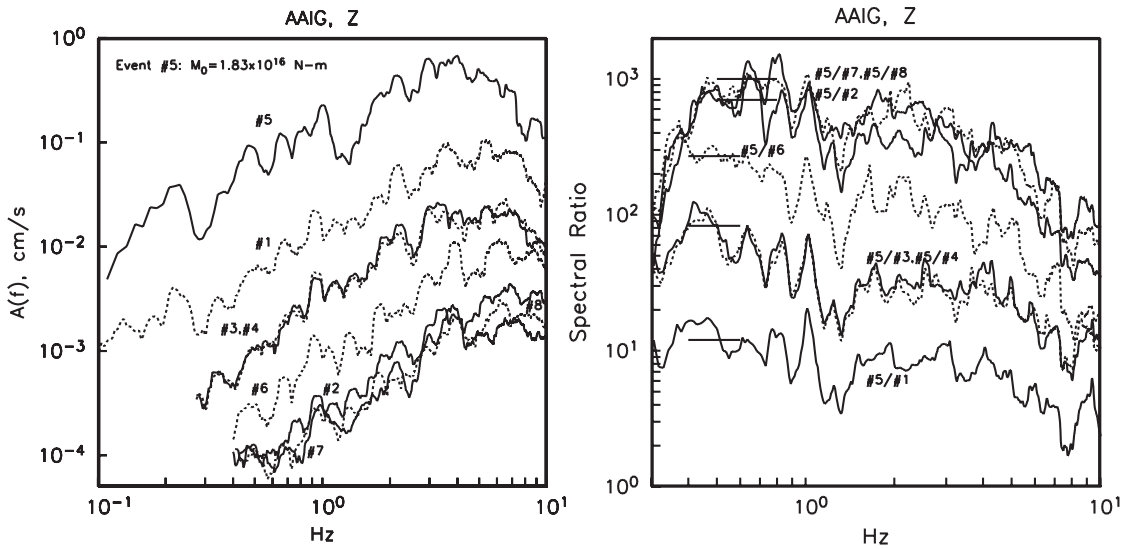

Figure 5. (Left) Fourier acceleration spectra (*Z*-component) of eight earthquakes at station AAIG (Figure 1). (Right) Spectral ratios of May 11, 2016 event (M_w4.8) with respect to the other seven events. As the seismic moment of 11 May, 2016 is known (M_0 = 1.83x10^{16} Nm), the ratios at low frequencies yield an estimate the moment (hence M_w) of the other seven events (Table 1).

$$A(f,R) = C \cdot G(R)\,[\{f^2 \dot{M}_0(f)\} Site(f) e^{-\pi\kappa f} B(f)]\,[e^{-\pi f R/\beta Q(f)}] \quad (1)$$

where,

$$C = FPR_{\theta\varphi}(2\pi)^2/(4\pi\rho\beta^3). \quad (2)$$

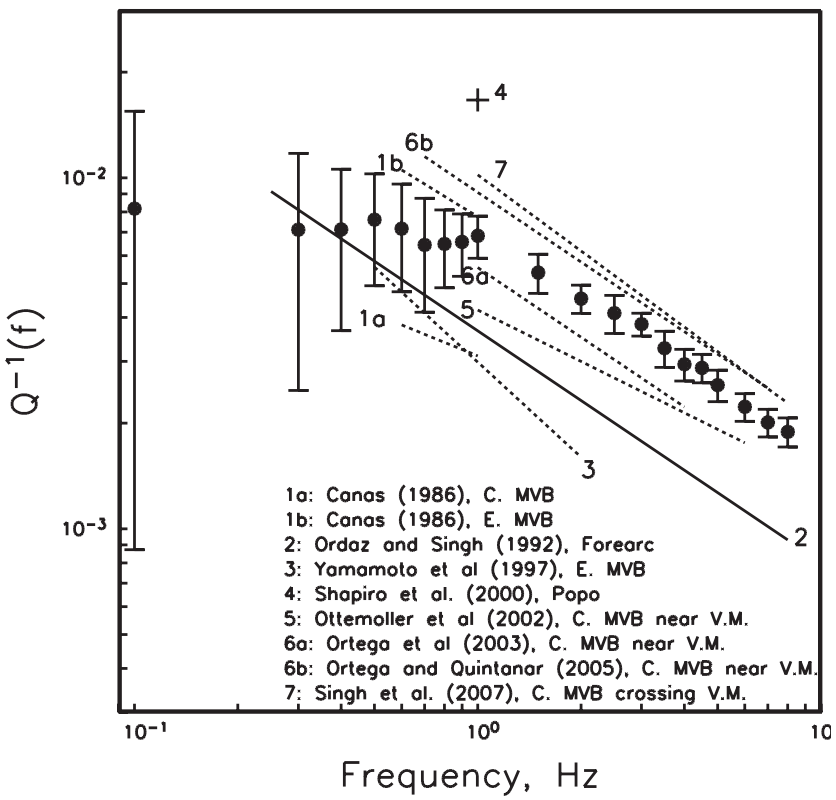

Figure 6. $Q^{-1}(f)$ of central-west TMVB estimated in this study (dots) and in other segments of TMVB reported in previous works. For comparison, Q^{-1} of *Lg* waves in the forearc region is also shown. Modified from Singh *et al*. (2007).

In equations above, $\dot{M}_0(f)$ is the moment rate spectrum so that $\dot{M}_0(f) \rightarrow M_0$ (the seismic moment) as $f \rightarrow 0$, R = hypocentral distance, $R_{\theta f}$ = average radiation pattern (0.55), F = free surface amplification (2.0), P takes into account the partitioning of energy in the two horizontal components ($1/\sqrt{2}$), b = shear-wave velocity at the source (taken here as 3.5 km/s), r = density in the focal region (assumed 2.85 g/cm^3), and $Q(f)$ = quality factor, which includes both anelastic absorption and scattering. The attenuation in the near-surface layer and the finite bandwidth of the observed spectrum imposed by the sampling rate are accounted by the parameter κ (Singh *et al*., 1982; Anderson and Hough, 1984) and/or the Butterworth filter, $B(f)$. Following Boore (1983), we take $B(f) = (1.0 + (f/f_m)^8)^{-0.5}$. We will assume that κ is independent of R. *Site* (f) in Equation (1) is the local site effect. We take the geometrical spreading term, $B(R)$, in Equation (1) as 1 / R for $R \leq$ 100 km and 1 / $(100R)^{0.5}$ for $R >$ 100 km. Taking logarithm of Equation (1) yields:

$$\log[A(f,R)] = \log C + \log G(R) + [\log\{f^2 \dot{M}_0(f)\} + \log B(f) + \log Site(f) - 1.36\kappa f] - [1.36\{Rf/\beta Q(f)\}]. \quad (3)$$

The terms in the first square bracket on the right-hand side depend on f but are independent of distance R. Equation (3) was solved in the least squares sense to obtain $Q^{-1}(f)$ and the quantity in the first square bracket at each frequency. Isolating the source acceleration spectrum, $f^2 \dot{M}_0(f)$ would require knowledge of *Site*(f), κ, and f_m. Here the only interest is Q^{-1}. Figure 6 shows Q^{-1} as a function of f. A least squares fit to the data in the frequency range 1 – 8 Hz yields $Q(f) = 141f^{0.63}$. The figure also shows $Q^{-1}(f)$ for the TMVB reported in previous studies and that obtained by Ordaz and Singh (1992) for interplate earthquakes in the forearc region of Mexico. As expected, a stronger attenuation (low Q) is, generally, observed in the TMVB than in the forearc region. However, as mentioned earlier, there is a large variation in the reported $Q^{-1}(f)$ in the TMVB. This may partly reflect smaller scale variation in the attenuation. Unfortunately, there are large differences in the reported $Q^{-1}(f)$ for the same region also (see, e.g., the values reported for the central or the eastern MVB in Figure 6). Thus, the variability in the reported $Q^{-1}(f)$ is partly also due to the difference in the data set as well as the methodology used in the analysis.

Ground motion in Guadalajara during larger, postulated earthquakes

Observed *PGA*, *PGV*, and *PGD* at GDLP and GDLC during the Guadalajara sequence are plotted as a function of M_w in Figure 7. It is clearly of practical interest to estimate these ground motion parameters for postulated larger earthquakes which may occur in the same source region. Here the motions from $M_w \leq 6.0$ events are estimated. The occurrence of a M_w5.5-6.0 earthquake in the same source region as the sequence or within R~20 km from the center of Guadalajara certainly does not seem farfetched. The San Cristóbal de la Barranca town, which suffered destruction (García Acosta and Suárez Reynoso, 1996) during the 11 February, 1875 earthquake is ~ 30 km NNE of the source region present sequence. The region is seismically active

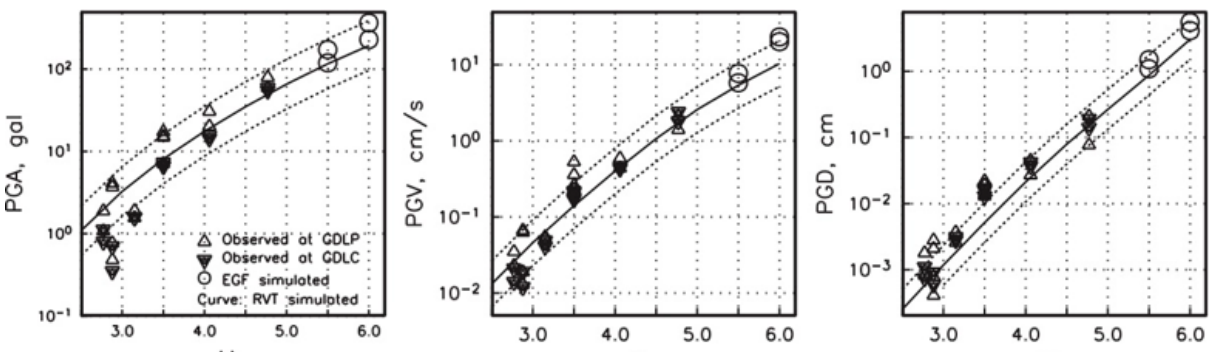

Figure 7. Observed, horizontal *PGA*, *PGV*, and *PGD* at stations GDLP and GDLC, located in Guadalajara (R~20 km), as a function of M_w. The curve shows prediction from RVT (see text). Circles indicate synthesized peak motions for postulated earthquakes of M_w5.5 and 6.0 using recordings of 15 December, 2015 (M4.1) as empirical Green's functions.

with potential for large earthquakes; thus it is relevant to estimate plausible ground motions during the scenario earthquakes. In this paper, two techniques were used, one based on random vibration theory (RVT) and the other exploiting summation of empirical Green's functions (EGFs).

Estimation based on RVT

If the Fourier's acceleration amplitude spectrum $A(f, R)$ and duration of the intense ground motion at a site can be estimated, then the peak ground motion parameters can be obtained through the application of RVT (see Boore, 2003 for an extensive review of the method). Here, $A(f, R)$ was estimated using Equation (1). We assume that the sources follow Brune ω^{-2} model, i.e.,

$$\dot{M}_0(f) = M_0 f_c^2/(f^2 + f_c^2),$$

where M_0 is the seismic moment, and f_c is the corner frequency which is related to the source radius, a, by $f_c = 2.34\beta / 2\pi a$ (Brune, 1970). The radius, in turn, is related to stress drop, $\Delta\sigma$, by $\Delta\sigma = (7/16)(M_0/a^3)$. We further assume that $\Delta\sigma$ is constant and equals 100 bar. As estimated above, we take $Q(f) = 141f^{0.63}$. An inspection of spectra at stations GDLP and GDLC suggest f_m = 18 Hz. The high-frequency fall off of the observed spectra additionally requires κ = 0.01 s. The spectrum was first computed using the parameters above and Equation (1) but neglecting the site amplification term, i.e., assuming *Site*(f) = 1. The ratio of observed to the computed spectrum yields an estimate of *Site*(f). The process is illustrated in figures 8a and 8b which show median and plus/minus one standard deviation curves of the observed horizontal spectra at stations GDLP and GDLC for 15 December, 2015 (M_w4.1) and 11 May, 2016 (M_w4.8) earthquakes, respectively. The figures also show the computed spectrum assuming *Site* (f) =1. The ratio of the observed median spectrum to the computed spectrum, *Site*(f), is shown in Figure 8c for the two events, along with the median *Site*(f). We use the median *Site*(f) in Equation (1) to estimate median $A(f,R)$ at stations GDLP and GDLC. A critical parameter needed in the application of RVT is the duration of intense part of the ground motion, T_s, which was taken as $T_s = 1/f_c + 0.05R + C$, where R is in km. We take C = 3.0 based on an earlier analysis of an earthquake sequence in Morelia (Singh *et al*., 2012). we note that C = 0 in the relation proposed by Herrmann (1985). The predicted *PGA*, *PGV*, and *PGD* curves as a function M_w are shown in Figure 7. The dashed curves in the figure correspond to twice and half the predicted RVT curve. These curves bracket most of the observed data. From RVT simulation, the expected *PGA*, *PGV*, and *PGD* at the accelerographic stations from a M_w6.0 earthquake in the source region of the sequence with $\Delta\sigma$ = 100 bar are 195 cm/s^2, 10 cm/s, and 3 cm, respectively. The computations with $\Delta\sigma$ = 30 bar and 300 bar were repeated. The estimated values fall between the dashed curves in Figure 7. Assuming 30 to 300 bar as the likely range for the stress drop, then the dashed curves in Figure 7 provide the range of the expected peak values.

Estimation based on random summation of empirical Green's function

The recordings of a smaller earthquake can be used as empirical Green's functions (EGFs) to synthesize expected ground motions during a postulated larger earthquake in the same source region. Here we use the recorded motion at the station GDLP during the 15 December, 2015 earthquake (M_w4.1) as the EGF. We follow method proposed by Ordaz *et al*. (1995) which assumes that far-field and point-source approximations are valid. The summation scheme obeys the ω^2-source scaling law at all frequencies and produces realistic time histories. The method requires specification of only the seismic moments and the stress drops of the EGF and the target events. Here we assume the same stress drop, $\Delta\sigma$, for the EGF and target events and take it as 100 bar. Figure 7 shows synthesized peak ground motions on NS and EW components (average of 30 simulations) for the postulated M_w 5.5 and 6.0 earthquakes. The peak values follow the trend of the recorded data and are in agreement, within a factor of two, with the RVT predictions. Simulated motions assuming $\Delta\sigma$ of 30 and 300 bar are, generally, lower and higher by about 20 to 40%, respectively.

The EGF recordings and sample simulated time histories corresponding M_w5.5 and 6.0 earthquakes are displayed in Figure 9. The simulated traces appear realistic. They provide an estimate of expected ground motions in the center of Guadalajara during these scenario earthquakes.

Discussion and Conclusions

The similarity of waveforms and constant (*S-P*) time of 2.5 s at the accelerographic station GDLP for all well-recorded eight events of the earthquake sequence suggest that the activity was confined to a small volume, probably about 1 to 2 km in radius, and the focal mechanisms were nearly the same. The

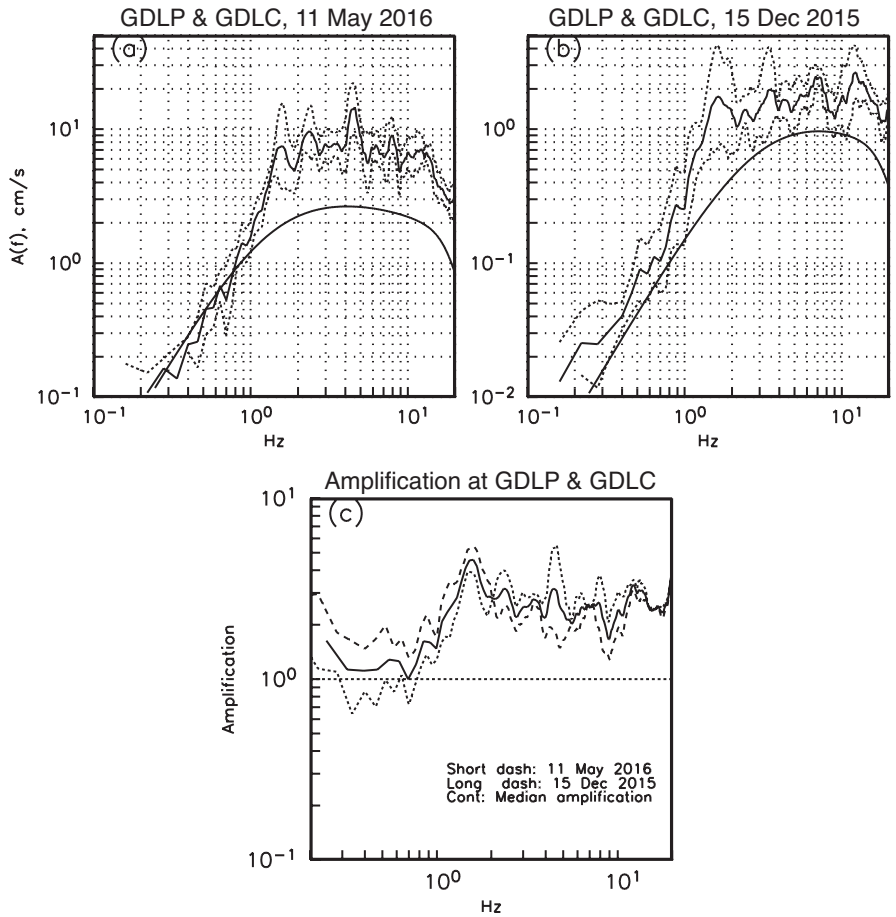

Figure 8. (a) Median and plus/minus one standard deviation of observed Fourier acceleration spectra (horizontal components) at stations GDLP and GDLC during the 11 May, 2016 (M_w4.8) earthquake. Also shown are corresponding theoretical spectra assuming ω^{-2} Brune source model with $\Delta\sigma$ = 100 bar, $Q(f)$ = 141$f^{0.63}$, f_{max} = 18 Hz, and κ = 0.01 s and ignoring the site effect. (b) Same as (a) but for the 15 December, 2015 (M_w4.1) earthquake. An estimation of median site effect at stations GDLP and GDLC is obtained from the ratio of observed to theoretical spectra. (c) Estimated site effects during 15 December, 2015 and 11 May, 2016 earthquakes. The continuous curve shows the median site effect.

focal mechanism of the largest earthquake of the sequence (11 May, 2016; M_w4.8) reveals normal-faulting on a NNE-SSW oriented fault, with a nearly horizontal *T* axis trending ~ 110º. This mechanism is not consistent with the NE-SW direction of motion measured on fault strike by Barrier *et al*. (1990) ~ 35 km WNW of Guadalajara.

The sequence occurred in a region where Sierra Madre Occidental volcanic province abuts the TMVB. About 80 km north of Guadalajara, near the town of Teul, large NNE trending 22 – 27 Ma old normal faults have been mapped (Moore *et al*., 1994). -N-S trending normal faults (age < 10 Ma) are found about 50 km north of Guadalajara near the town of San Cristóbal. According to Moore *et al*. (1994) the trend of these faults suggests a reactivation of older Basin and Range structures. It is possible that the present earthquake sequence occurred on one these reactivated structures.

From an analysis of the recordings of the largest event of the sequence, we obtain an estimate of the attenuation parameter, Q, in the central-west TMVB as Q = 141$f^{0.63}$. We note that this estimate is preliminary, as it is based on only one event. However, given the uncertainty in the regression, the trend is not expected to change appreciably if, and when, more data are available and are included in a similar analysis. Previous estimations of Q in the TMVB have been limited to the central and eastern segments. They differ significantly among the studies. The present Q estimate is

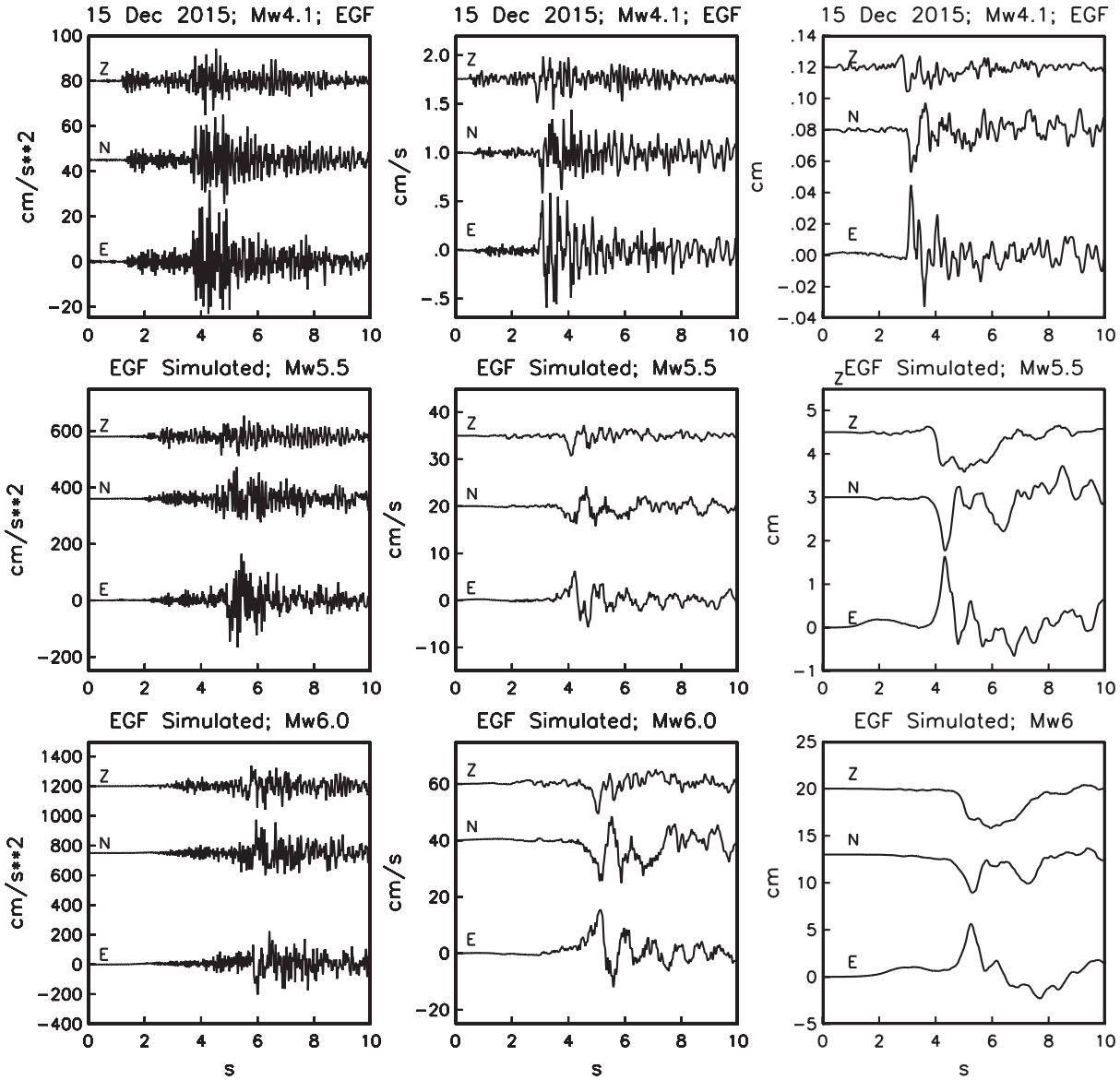

Figure 9. (Top frames) Acceleration, velocity, and displacement traces at station GDLP during the 15 December, 2015 earthquake used as EGFs. (Middle frames) Synthesized motions for a postulated M_w5.5 earthquake. (Bottom frames) Synthesized motions for a postulated M_w6.0 earthquake. Stress drops of the EGF and target events have been taken as 100 bar. Sample time histories are one realization of the synthesis.

somewhat higher than those reported in the central TMVB for paths crossing the Valley of Mexico. The Q reported here is an average over a 650 km-long path; it may be much lower for short paths crossing active volcanoes. Almost all Q estimates for the TMVB are smaller than that in the forearc region of Mexico. Lower Q (higher attenuation of seismic waves) in the TMVB may be attributed to heating and partial melting of crustal material, presence of fluids, and enhanced scattering from heterogeneities and fractures resulting from active tectonics of the volcanic belt.

Damage caused by large historical earthquakes of 1568 and 1875 are a testimony to the seismic hazard faced by Guadalajara. The causative faults of these events, however, are not known and the magnitudes are uncertain. There is also infrequent seismic activity at a small-magnitude level in the city. Ordoñez (1912) reported a swarm-like local seismic activity. Whether the activity in the city is diffused or confined to some structures is unknown. As a result of these uncertainties, scenario earthquakes for the city are difficult to postulate. Clearly, a dense

seismic network is needed in and around the metropolitan area of Guadalajara which has a population of about 4.5 million. Such a network, along with paleoseismic studies, may go a long way in identifying active faults in the region and, hence, in realistic estimation of seismic hazard. In this study, we have taken advantage of the strong motion recordings in Guadalajara during the recent seismic sequence and have estimated ground motions from $M_w \leq 6$ scenario earthquakes in the same source region. The ground motion estimates obtained from RVT and EGF techniques are in reasonable agreement with each other. These are some of the likely scenario earthquakes. The parameters used in the simulation were obtained from the strong-motion recordings. They could also be useful in the simulation of motions from other postulated scenario earthquakes.

Acknowledgments

SSN data were obtained by the Servicio Sismológico Nacional (México) and accelerographic data from Guadalajara were provided by Instrumentación Sísmica, Instituto de Ingeniería, UNAM. We especially thank the personnel of both of these institutions for station maintenance, data acquisition, transmission, processing, and distribution. The research was partly funded by DGAPA, UNAM project IN107216.

References

Allan J.F., Nelson S.A., Luhr J.F., Carmichael I.S.E., Wopat M., Wallace P.J., 1991, Pliocene-recent rifting in SW Mexico and associated Volcanism: An exotic terrain in the making. In: Dauphin, J.P., Simoneit, B.R.T., (Eds.), *The Gulf and the Peninsular Province of the Californias*, *AAPG Mem.*, 47, 425-445.

Anderson J.G., Hough S.E., 1984, A model for the shape of the Fourier amplitude spectrum of acceleration at high frequencies. *Bull. Seismol. Soc. Am.*, 74, 5, 1969-1993.

Barrier E., Bourgois J., Michaud F., 1990, Le sisteme de rifts actifs du point triple de Jalisco: vers un proto-golfe de Jalisco. *C.R. Acad. Sci. Paris,* 310, 1513-1520.

Boore D.M., 1983, Stochastic simulation of high-frequency ground motions based on seismological models of radiated spectra. *Bull. Seism. Soc. Am.,* 73, 1865-1884.

Boore D.M., 2003, Simulation of ground motion using the stochastic method. *Pageoph,* 160, 635-676.

Brune J.N., 1970, Tectonic stress and the spectra of seismic shear waves from earthquakes. *J. Geophys. Res.,* 75, 4997-5009.

Camacho H., Flores T., 1922, Memoria relativa al Terremoto Mexicano del 3 de Enero de 1920. *Boletín del Instituto de Geológico de México*, 38-39.

Campillo M., Singh S.K., Shapiro N., Pacheco J., Hermann R.B., 1996, Crustal structure of the Mexican volcanic belt, based on group velocity dispersion. *Geofísica Internacional*, 35, 4, 361-370.

Canas J.A., 1986, Estudio de factor inelástico Q de la coda de los terremotos correspondientes a las regions central y oriental del eje volcánico de México. *Geofísica Internacional*, 25, 503-520.

Dreger D.S., 2003, TDMT_INV: Time Domain Seismic Moment Tensor INVersion, *International Handbook of Earthquake and Engineering Seismogy*, 81B, 1627.

García D., Singh S.K., Herráiz H., Pacheco J.F., Ordaz M., 2004, Inslab earthquakes of central Mexico: Q, source spectra and stress drop. *Bull. Seism. Soc. Am.,* 94, 789-802.

García Acosta V., Suárez Reynoso G., 1996, Los sismos en la historia de México, tomo I. FCE, UNAM, CIESAS, Mexico City, 718 pp.

Havskov J., Ottemöller L., 1999, Electronic seismologist: SeisAn earthquake analysis software. *Seism. Res. Lett.,* 70, 532-534.

Herrmann R.B., 1985, An extension of random vibration theory estimates of strong ground motion at large distances. *Bull. Seism. Soc. Am.,* 75, 1447-1453.

Johnson C.A., Harrison C.G.A., 1990, Neotectonics in Central Mexico. *Phys. Earth Planet. Int.*, 64, 187-210.

Lienart B.R., Havskov J., A computer program for locating earthquakes both locally and globally, *Seism. Res. Lett.*, *66*, 26-36, 1995.

Michaud F., Bourgois J., Parrot J.F., Taud H., Kasser M., 1994, Le point triple de Jalisco (Mexique): évolution tectonique á partir du traitement do données MNT-SPOT. *C. R. Acad. Sci. Paris*, 318, 1117-1124.

Moore G., Marone C., Carmichael I.S.E., Renne P., 1994, Basaltic volcanism and extension near the intersection of the Sierra Madre

volcanic province and the Mexican Volcanic Belt.*Geol. Soc. Am. Bull.*, 106, 383-394.

Ordaz M., Singh S.K., 1992, Source spectra and spectral attenuation of seismic waves from Mexican earthquakes, and evidence of amplification in the hill zone of Mexico City. *Bull. Seism. Soc.Am.*, 82, 24-43.

Ordaz M., Arboleda J., Singh S.K., 1995, A scheme of random summation of an empirical Green´s function to estimate ground motions from future large earthquakes. *Bull. Seism. Soc. Am.*, 85, 1635-1647.

Ordoñez E., 1912, The recent Guadalajara earthquakes. *Bull. Seism. Soc. Am.*, 2, 134-137.

Ortega R., Quintanar L., 2005, A study of local magnitude scale in the Basin of Mexico: Mutually consistent estimate of logA0 and ground motion scaling. *Bull. Seism. Soc. Am.*, 95, 605–613.

Ortega R., Herrmann R.B., Quintanar L., 2003, Earthquake groundmotion scaling in central Mexico, *Bull. Seism. Soc. Am.*, 93, 397–413.

Ottemöller L., Shapiro N.M., Singh S.K., Pacheco J.F., 2002, Lateral variation of Lg wave propagation in southern Mexico. *J. Geophys. Res.*, 107 (B1), doi: 10.1029/2001JB000206

Pacheco J.F., Mortera C., Delgado H., Singh S.K., Valenzuela R.W., Shapiro N.M., Santoyo M.A., Hurtado A., Barrón R., Gutiérrez E., 1999, Tectonic significance of an earthquake sequence in the Zacoalco half-graben, Jalisco, Mexico. *J. South American Earth Sciences*, 12, 557-565.

Pasquaré G., Vezzoli L., Zanchi A., 1987, Morphological and structural model of Mexican Volcanic Belt, *Geofísica Internacional*, 26, 159-176.

Shapiro N.M., Singh S.K., Iglesias-Mendoza A., Cruz-Atienza V.M., Pacheco J.F., 2000, Evidence of low Q below Popocateptl volcano and its implications to seismic hazard in México City, *Geophys. Res. Lett.*, 27, 2753–2756.

Singh S.K., Apsel R., Fried J., Brune J.N., 1982, Spectral attenuation of SH-wave along the Imperial fault. *Bull. Seism. Soc. Am.*, 72, 2003-2016.

Singh S.K., Ordaz M., Pacheco J.F., Courboulex F., 2000, A simple source inversion scheme for displacement seismograms recorded at short distances. *J. Seismology*, 4, 267-284, 2000.

Singh S.K., Iglesias A., García D., Pacheco J.F., Ordaz M., 2007, *Q* of *Lg* waves in the Central Mexican Volcanic Belt.*Bull. Seism. Soc. Am.*, 97, 1259-1266.

Singh S., Iglesias A., Garduño V.H., Quintanar L., Ordaz M., 2012, A source study of the October, 2007 earthquake sequence of Morelia, Mexico and ground-motion estimation from larger earthquakes in the region. *Geofísica internacional*, 51, 1, 73-86.

Suárez G., García-Acosta V., Gaulon R., 1994, Active crustal deformation in the Jalisco block, Mexico: evidence for a great historical earthquake in the 16th century. *Tectonophysics*, 234*,* 1, 117-127.

Suter M., López-Martínez M., Quintero Legorreta O., Carrillo-Martínez M., 2001, Quaternary intra-arc extension in the central Trans-Mexican Volcanic Belt. *GSA Bulletin*, 113, 693–703.

UNAM Seismology Group, 2010, Intraslab Mexican earthquakes of 27 April 2009 (M_w5.8) and 22 May 2009 (M_w5.6): a source and ground motion study. *Geofísica Internacional*, 49, 153-163.

Urbina F., Camacho H., 1913, La zona megaseísmica Acambay-Tixmadejé. Estado de México, conmovida el 19 noviembre 1912. *Bol. Inst. Geol. Méx.*, 32, 125 pp.

Yamamoto J., Quintanar L., Herrmann R.B., Fuentes, C., 1997, Lateral variations of Lg coda Q in southern Mexico. *Pageoph*, 149, 3, 575-599.

Zúñiga F.R., Pacheco J.F., Guzmán-Speziale M., Aguirre-Dıaz G.J., Espíndola V.H., Nava E., 2003, The Sanfandila earthquake sequence of 1998, Queretaro, Mexico: activation of an undocumented fault in the northern edge of central Trans-Mexican Volcanic Belt. *Tectonophysics*, 361, 3, 229-238.